Cathodoluminescence studies of electron injection effects in p-type Gallium Oxide

Leonid Chernyak, Alfons Schulte, Jian-Sian Li, Chao-Ching Chiang, Fan Ren, Stephen J Pearton, Corinne Sartel, Vincent Sallet, Zeyu Chi, Yves Dumont, et al.

Cathodoluminescence studies of electron injection effects in p-type Gallium Oxide

Leonid Chernyak [1, a)], Alfons Schulte [1], Jian-Sian Li [2], Chao-Ching Chiang [2], Fan Ren [2], Stephen J. Pearton [3], Corinne Sartel [4], Vincent Sallet [4], Zeyu Chi [4], Yves Dumont [4], Ekaterine Chikoidze [4], and Arie Ruzin [5]

[1] *Department of Physics, University of Central Florida, Orlando, FL 32816, USA*

[2] *Department of Chemical Engineering, University of Florida, Gainesville, FL 32611, USA*

[3] *Material Science and Engineering, University of Florida, Gainesville, FL 32611, USA*

[4] *Groupe d'Etude de la Matière Condensée, Université Paris-Saclay, Université de Versailles Saint Quentin en Yvelines – CNRS, 45 Av. des Etats-Unis, 78035 Versailles Cedex, France*

[5] *School of Electrical Engineering, Tel Aviv University, Tel Aviv 69978, Israel*

It was recently demonstrated that electron beam injection into p-type β-Gallium Oxide leads to a significant linear increase of minority carrier diffusion length with injection duration, followed by its saturation. The effect was ascribed to trapping of non-equilibrium electrons (generated by a primary electron beam) on meta-stable native defect levels in the material, which in turn blocks recombination through these levels. In this work, in contrast to previous studies, the effect of electron injection in p-type Ga_2O_3 was investigated using cathodoluminescence technique *in-situ* in Scanning Electron Microscope, thus providing insight on minority carrier lifetime behavior under electron beam irradiation. The activation energy of ~ 0.3 eV, obtained for the phenomenon of interest, is consistent with the involvement of Ga vacancy-related defects.

[a)] Author to whom correspondence should be addressed: chernyak@physics.ucf.edu

I. Introduction

Electron injection plays a critical role in manipulating minority carrier transport within semiconductors, particularly in ultra-wide-bandgap materials such as Gallium Oxide, which is becoming increasingly important for high-power and advanced optoelectronic devices [1-6]. In a semiconductor, the majority carriers are the charge carriers that naturally dominate conduction (electrons in n-type and holes in p-type). Minority carriers, on the other hand, are the opposite type and exist in much lower concentrations. However, their transport properties are crucial for the functionality of bipolar devices.

One of the most significant effects of electron injection is its ability to extend the minority carrier diffusion length [7]. This length represents the average distance a minority carrier can travel before recombining with a majority carrier. This recombination process effectively eliminates the minority carrier from contributing to conduction.

Electron injection can positively impact diffusion length by "passivating" recombination centers [7]. These centers are microscopic defects within the semiconductor lattice that act as traps for majority and minority carriers. By filling these traps, electron injection essentially reduces the availability of recombination sites. Consequently, minority carriers have a higher probability of surviving longer and traveling further before encountering a recombination event, leading to an increased diffusion length.

Impact of electron injection on minority carrier diffusion length, due to irradiation with 10-20 keV electron beam of a scanning electron microscope (SEM), was recently studied in n- and highly resistive p-type *β-Ga_2O_3/c-sapphire* films with (-201) preferential orientation [8, 9]. The effect was ascribed to trapping of non-equilibrium electrons [10], generated by the primary SEM electron beam, on native defects-associated metastable levels in the bandgap of Ga_2O_3. In this work, the

increase of minority carrier diffusion length in *homoepitaxial* p-type (010)-oriented Ga_2O_3 layers was studied under electron beam irradiation and was complemented with cathodoluminescence emission from the same region, providing insight for the mechanism of the phenomenon.

In contrast to the previous reports [8, 9] on studies of electron injection effects in Ga_2O_3, in which Electron Beam-Induced Current (EBIC) technique *in-situ* in SEM was predominantly used, this work focused on variable temperature cathodoluminescence (CL) studies, thus shading light on lifetime of non-equilibrium carriers. Additionally, in the present work, the two independent techniques – EBIC and CL – were correlated, to better understand the relationship between the minority carrier diffusion length and lifetime.

II. Experimental

Undoped 1 μm-thick β-Ga_2O_3 was grown on (010)-oriented insulating Fe-doped Ga_2O_3 in a RF-heated horizontal metalorganic chemical vapor deposition (MOCVD) reactor using Ga/O ratio and growth temperature of 1.4×10^{-4} and 775 °C, respectively [11, 12]. X-ray diffraction revealed high quality layer of β-Ga_2O_3 with monoclinic space group (*C2/m*) symmetry.

Metal contacts for electrical characterization were prepared by Ti/Au deposited at the four corners of the sample in a Van der Pauw configuration. The contacts were tested by measuring I-V characteristics, which showed the Ohmic dependence in the temperature range of 450-850 K. Because the contacts exhibited deviation from the linear I-V dependence below 450 K, the Hall effect measurements were not conducted at room temperature. The positive Hall voltage increased with increasing magnetic field, thus confirming the *p*-type nature of the epitaxial layer with hole concentration $p \sim 2\times10^{17}$ cm^{-3} and resistivity $\rho \sim 0.39$ Ω·cm at 450 K. Detailed studies of electrical properties for the epitaxial layer under test will be outlined in a separate article under preparation.

Minority carrier diffusion length, L, measurements were carried out using Electron Beam-Induced Current technique *in-situ* in Phillips XL-30 SEM using planar line-scan electron beam excitation with an electron beam moving along the sample's surface [7, 10, 13, 14]. The EBIC measurements were carried out at room temperature under an electron beam accelerating voltage of 20 kV (to cover the whole epitaxial layer thickness), corresponding to ~ 0.6 nA absorbed current (measured with Keithley 480 picoammeter) and ~ 1 μm electron range (penetration depth) in the material [14]. The EBIC line-scans (16.3 μm lateral length) for diffusion length extraction were carried out using Ni/Au (20 nm/80 nm) asymmetrical pseudo-Schottky contacts created on the film with lithography/liftoff techniques.

A single line-scan takes approximately 12 seconds, which is sufficient for extraction of minority carrier diffusion length value from the exponential decay of Electron Beam-Induced Current in agreement with the following equation:

$$I(x) = I_0 x^{\alpha} \exp\left(-\frac{x}{L}\right) \qquad (1)$$

Here, $I(x)$ is the Electron Beam-Induced Current signal as a function of coordinate; I_0 is a scaling factor; x is the coordinate measured from the edge of the contact (Ni/Au) stack; α is a recombination coefficient (set at -0.5).

To perform electron injection in the region of EBIC measurements, line-scans were not interrupted for the total time of up to ~ 1200 seconds (corresponding to the primary excitation electron charge density of 3.2×10^{-7} C/μm^3). The values of diffusion length were periodically extracted using equation (1) for different incremental durations of electron injection varying from nearly zero (for the first line-scan) to 1200 seconds. EBIC signal was amplified with Stanford Research Systems SR 570 low-noise current amplifier and digitized with Keithley DMM 2000, controlled by a PC using home-made software.

It should be noted that the primary excitation SEM electron beam serves for generation of non-equilibrium electron-hole pairs in the material due to the band-to-band (valence band to conduction band) transition of excited electrons. The primary excitation electrons do not accumulate in the material since the sample is grounded, thus preserving the sample's electroneutrality.

Cathodoluminescence (CL) measurements were carried out in 300-330 K temperature range under 20 kV accelerating voltage using Gatan MonoCL2 attachment to the SEM integrated with a variable temperature stage and an external controller. Spectra were recorded with a Hamamatsu photomultiplier tube sensitive in 150-850 nm range and single grating monochromator (blazed at 1200 lines/mm) [15].

III. Results and discussion

Fig. 1 demonstrates a series of room temperature continuous CL spectra from the 10 μm^2 area on the surface of Gallium Oxide as function of electron beam irradiation duration (see above for the electron beam injection regimes). The observed CL spectra are typical for Ga_2O_3 and instead of showing the near band edge emission, they consist of several broad emission bands. The origins of broad emission bands in β-Ga_2O_3 include complexes of O and Ga vacancies, O-related complexes and O and Ga interstitials. Detailed studies of n- and p-type Ga_2O_3 optical properties were recently presented in refs. [13, 16]. It could be seen from the spectra in Fig. 1, that the CL intensity shows a continuous decrease with electron irradiation duration ranging from nearly zero (less than 20 seconds time difference; spectrum 1) to 1440 seconds (spectrum 4).

The peak intensity for each spectrum, presented in Fig. 1 at room temperature, was correlated in Fig. 2 with the minority carrier diffusion length, measured as a function of electron beam

irradiation duration in the same area of Ga_2O_3. In agreement with the previous studies for n- and highly resistive hetero-epitaxially grown p-type Ga_2O_3 [8, 9], minority carrier diffusion length in Fig. 2 exhibits a linear increase (before saturation) consistent with a decrease of peak CL intensity. The mechanism responsible for the effects in Fig. 2 is detailed in refs. [8, 9, 16, 17] and is ascribed to trapping of non-equilibrium carriers, generated by the primary electron beam, on native defect levels in the forbidden gap.

A non-equilibrium electron, generated by a primary scanning electron microscope beam, gets trapped by deep levels in Ga_2O_3 [8, 9]. Because of a relatively "deep" energetic position in the Ga_2O_3 forbidden gap, a pronounced number of these defects remains in the neutral state, thus acting as meta-stable electron traps. Although the exact number of neutral traps in Gallium Oxide is unknown, it is logical to assume it to be comparable with that in GaN ($\sim 10^{18}$ cm^{-3} [17]). Trapping non-equilibrium electrons on the defect levels (traps) in the forbidden gap of Gallium Oxide prevents additional recombination of the conduction band electrons through these levels. This leads to an increase of lifetime, τ, for non-equilibrium electrons in the conduction band and, as a result, to an increase of minority carrier diffusion length, L, in agreement with the equation (2).

$$L = \sqrt{D\tau} \qquad (2)$$

In equation (2), D represents a diffusion coefficient for minority carriers, which is unaffected by electron irradiation [15].

Because L depends linearly (cf. Fig. 2) on duration of electron irradiation, t, the CL peak intensity, I (not to be mixed with the EBIC signal $I(x)$) which is proportional to τ^{-1} [18], should depend on duration proportional to $1/t^2$, in agreement with the equation (2). This is, indeed, observed in Fig. 2. As $\tau \sim I^{-1}$ and $\sqrt{\tau}$ depends linearly on t (cf. L dependence on t in Fig. 2), one should expect a linear dependence for $1/\sqrt{I}$ on electron irradiation duration. This dependence was

experimentally verified and is presented in Fig. 3 for the temperatures ranging from 293 to 333 K. A span for decay of the CL intensity diminishes at higher temperatures, as is shown in Fig. 3. The rate R for CL decay at each temperature was obtained from the slopes of linear dependencies. R versus T dependence for the sample under investigation, shown in the inset of Fig. 4, was fitted using the following equation [9]:

$$R = R_0 \, exp\left(\frac{\Delta E_A}{2kT}\right) \qquad (3)$$

In equation (3), R_0 is the scaling constant; ΔE_A is the process activation energy; k is the Boltzmann constant; T is temperature in Kelvin. ΔE_A for the CL intensity decay was obtained from the slope of the Arrhenius plot shown in Fig. 4. The best fit was obtained for ΔE_A = 309 meV.

Refs. [19, 20] summarize traps in Ga_2O_3, which are associated with native defects and impurities. According to [19], Gallium vacancy (V_{Ga}) – related energetic levels are located at 0.1-0.3 eV and 0.3-0.5 eV above the top of the valence band. In the previous work, focused on electron beam irradiation impact on minority carrier diffusion length in highly resistive p-type Ga_2O_3/c-sapphire [9], the activation energy around 0.1 eV was identified. The relative proximity of the activation energies obtained for the different samples and from the independent experimental techniques – EBIC in ref. [9] and CL in this work – suggests involvement of the same defect levels in both cases.

IV. Conclusions

In this work, variable temperature cathodoluminescence studies of undoped p-type Gallium Oxide epitaxial layer were carried out and correlated with minority carrier diffusion length measurements, using two independent CL and EBIC techniques, in the same region subjected to electron beam irradiation. Elongation of the diffusion length and a simultaneous CL intensity decay

(from the same region) with increasing duration of electron beam irradiation were ascribed to charge trapping on the deep metastable levels in Gallium Oxide forbidden gap, which leads, in turn, to a longer non-equilibrium minority carrier lifetime in the conduction band. The activation energy of ~ 0.3 eV, associated with the impact of electron beam irradiation (injection) on CL emission intensity, was ascribed to Gallium vacancy-related point defects. These defects don't necessarily determine the p-type electrical conductivity in the sample but play a significant role in the charge trapping effects. Relative proximity of the activation energies, previously obtained from the EBIC measurements for the highly resistive p-type Ga_2O_3 samples, and the CL measurements, carried out in this work, suggests similarity of involved defect levels in both cases.

Finally, the values for minority carrier (electrons) diffusion length obtained in this work (750 nm at nearly zero electron irradiation duration; 12 seconds difference), are almost a factor of 10 larger as compared to the diffusion length (~ 100 nm at room temperature) measured for Si-doped n-type Gallium Oxide epitaxial layers (5×10^{16} cm^{-3} – 2×10^{17} cm^{-3} majority electron concentration) [21, 22], thus providing additional evidence for a p-type conductivity in the sample under investigation.

Acknowledgements

The research at UCF was supported in part by NSF (ECCS2310285; ECCS2341747; ECCS 2427262), US-Israel BSF (award # 2022056) and NATO (awards # G6072; G6194). The work at UF was performed as part of the Interaction of Ionizing Radiation with Matter University Research Alliance (IIRM-URA), sponsored by the Department of the Defense, Defense Threat Reduction Agency under award HDTRA1-20-2-0002, monitored by Jacob Calkins. The present work is a part of "GALLIA" International Research Project, CNRS, France. GEMaC colleagues acknowledge

financial support of French National Agency of Research (ANR), project "GOPOWER", CE-50 N0015-01. Research at Tel Aviv University was partially supported by US-Israel BSF (award # 2022056) and NATO (awards # G6072).

Conflict of Interest

The authors have no conflict to disclose.

Data Availability

The data that supports the findings of this study is available within the article.

References

1. S.J. Pearton, J. Yang, P.H. Cary, F. Ren, J. Kim, M.J. Tadjer, and M.A. Mastro, *Appl. Phys. Rev.*, **5**, 011301 (2018).
2. J.Y. Tsao, S. Chowdhury, M.A. Hollis, D. Jena, N.M. Johnson, K.A. Jones, R.J. Kaplar, S. Rajan, C.G. Van de Walle, E. Bellotti, C.L. Chua, R. Collazo, M.E. Coltrin, J.A. Cooper, K.R. Evans, S. Graham, T.A. Grotjohn, E.R. Heller, M. Higashiwaki, M.S. Islam, P.W. Juodawlkis, M.A. Khan, A.D. Koehler, J.H. Leach, U.K. Mishra, R.J. Nemanich, R.C.N. Pilawa-Podgurski, J.B. Shealy, Z. Sitar, M.J. Tadjer, A.F. Witulski, M. Wraback, and J.A. Simmons, *Adv. Electron. Mater.*, **4**, 1600501 (2018).
3. H. von Wenckstern, *Adv. Electron. Mater.*, **3**, 1600350 (2017).
4. M. Kim, J.-H. Seo, U. Singisetti, and Z. Ma, *J. Mater. Chem.*, **C 5**, 8338 (2017).
5. M. Higashiwaki, K. Sasaki, H. Murakami, Y. Kumagai, A. Koukitu, A. Kuramata, T. Masui, and S. Yamakoshi, *Semicond. Sci. Technol.*, **31**, 034001 (2016).
6. A. Kuramata, K. Kimiyoshi, W. Shinya, Y. Yu, M. Takekazu, and Y. Shigenobu, *Jpn. J. Appl. Phys.*, Part 1, **55**, 1202A2 (2016).
7. L. Chernyak, A. Osinsky, and A. Schulte, *Solid-State Electronics*, **45**, 1687 (2001).
8. S. Modak, J. Lee, L. Chernyak, J. Yang, F. Ren, S.J. Pearton, S. Khodorov, and I. Lubomirsky, *AIP Advances*, **9**, 015127 (2019).
9. S. Modak, A. Schulte, C. Sartel, V. Sallet, Y. Dumont, E. Chikoidze, X. Xia, F. Ren, S.J. Pearton, A. Ruzin, and L. Chernyak, *Appl. Phys. Lett.*, **120**, 233503 (2022).
10. O. Lopatiuk-Tirpak, L. Chernyak, F.X. Xiu, J.L. Liu, S. Jang, F. Ren, S.J. Pearton, K. Gartsman, Y. Feldman, A. Osinsky, and P. Chow, *J. Appl. Phys.*, **100**, 086101 (2006).

11. Z. Chi, C. Sartel, Y. Zheng, S. Modak, L. Chernyak, C.M. Schaefer, J. Padilla, J. Santiso, A. Ruzin, A.M. Gonçalves, J. von Bardeleben, G. Guillot, Y. Dumont, A. Pérez-Tomás, E. Chikoidze, *Journal of Alloys and Compounds*, **969**, 172454 (2023).
12. Z. Chi, J.J. Asher, M.R. Jennings, E. Chikoidze, A. Pérez-Tomás, *Materials*, **15**, 1164 (2022).
13. S. Modak, L. Chernyak, A. Schulte, C. Sartel, V. Sallet, Y. Dumont, E. Chikoidze, X. Xia, F. Ren, S.J. Pearton, A. Ruzin, D.M. Zhigunov, S.S. Kosolobov, and V.P. Drachev, *APL Mater.*, **10**, 031106 (2022).
14. E.B. Yakimov, A.Y. Polyakov, I.V. Shchemerov, N. B. Smirnov, A.A. Vasilev, P.S. Vergeles, E.E. Yakimov, A.V. Chernykh, F. Ren and S.J. Pearton, *Appl. Phys. Lett.*, **118**, 202106 (2021).
15. L. Chernyak, W. Burdett, M. Klimov, A. Osinsky, *Appl. Phys. Lett.*, **82**, 3680 (2003).
16. S. Modak, L. Chernyak, A. Schulte, M. Xian, F. Ren, S.J. Pearton, A. Ruzin, S.S. Kosolobov, V.P. Drachev, *AIP Advances*, **11**, 125014 (2021).
17. S. Modak, L. Chernyak, M.H. Xian, F. Ren, S.J. Pearton, S. Khodorov, I. Lubomirsky, A. Ruzin, and Z. Dashevsky, *J. Appl. Phys.*, **128**, 085702 (2020).
18. J.I. Pankove, "Optical Processes in Semiconductors" (Prentive-Hall, Englewood Clifs, NJ, 1971).
19. M. Labed, N. Sengouga, C.V. Prasad, M. Henini, *Materials Today Physics*, **36**, 101155 (2023).
20. A.Y. Polyakov, N.B. Smirnov, I.V. Shchemerov, S.J. Pearton, F. Ren, A.V. Chernykh, P.B. Lagov, T.V. Kulevoy, *APL Mater.*, **6**, 096102 (2018).
21. A.Y. Polyakov, I.-H. Lee, N.B. Smirnov, E.B. Yakimov, I.V. Shchemerov, A.V. Chernykh, A.I. Kochkova, A.A. Vasilev, F. Ren, P.H. Carey, S.J. Pearton, *Appl. Phys. Lett.*, **115**, 032101 (2019).

22. S. Modak, L. Chernyak, A. Schulte, M. Xian, F. Ren, S.J. Pearton, I. Lubomirsky, A. Ruzin, S.S. Kosolobov, V.P. Drachev, *Appl. Phys. Lett.*, **118**, 202105 (2021).

Figure Captions

Fig. 1. Room temperature CL spectra from the sample under test as a function of eletron beam irradiation duration. Spectrum **1** corresponds to nearly zero duration (20 seconds difference); spectrum **2** – 600 seconds; spectrum **3** – 1020 seconds; spectrum **4** – 1440 seconds.

Fig. 2. Dependence of minority carrier (electron) diffusion length (left vertical axis) and peak CL intensity from spectra **1**-**4** in Fig. 1 (right vertical axis) on duration of electron beam irradiation at room temperature. Both EBIC and CL measurements were carried out in the same region subjected to electron beam irradiation.

Fig. 3. Impact of electron beam irradiation duration on inverse square root of normalized CL intensity at various temperatures. The rate *R* for CL decay at each temperature is obtained as the slope of the linear fit.

Fig. 4. Ahrrenius plot for the rate *R* as a function of temperature. The activation energy of 309 meV is obtained as a slope of the linear fit. **Inset**: *R* versus *T* dependence for the Gallium Oxide sample under test.

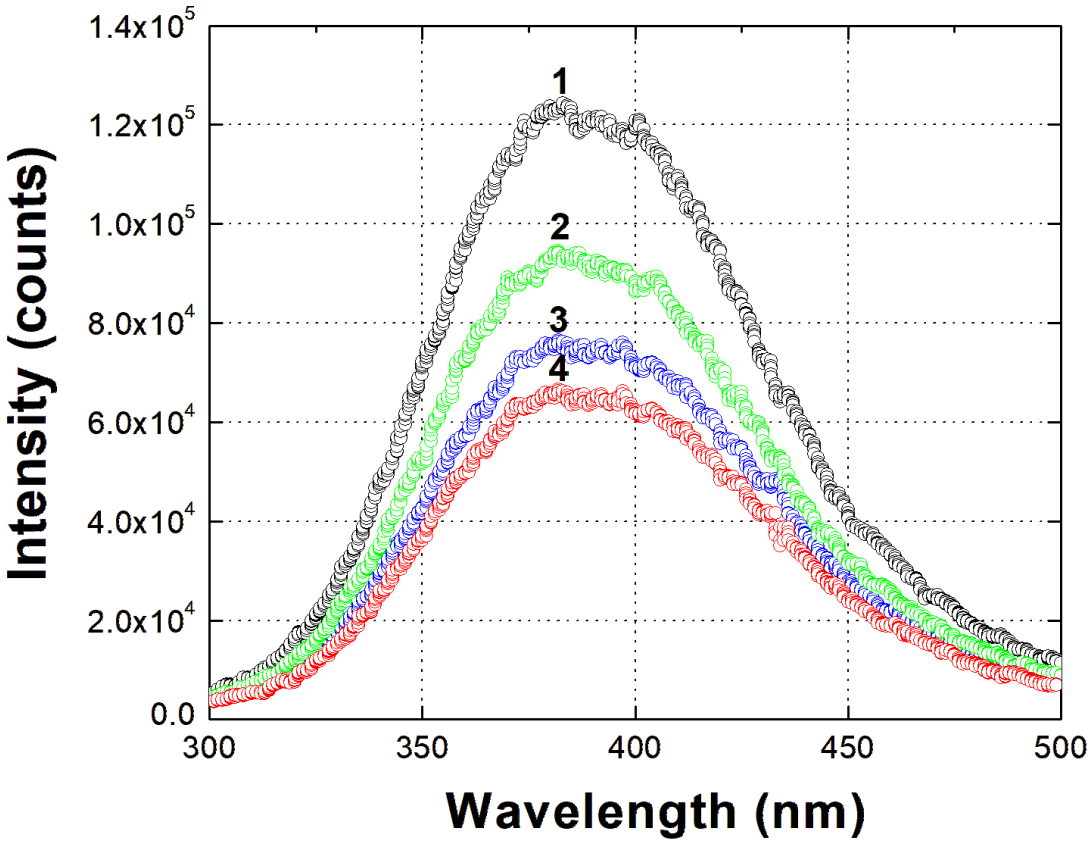
Intensity (counts)
1.4x10^5
1.2x10^5
1.0x10^5
8.0x10^4
6.0x10^4
4.0x10^4
2.0x10^4
0.0
300
350
400
450
500
Wavelength (nm)
1
2
3
4

Fig. 1

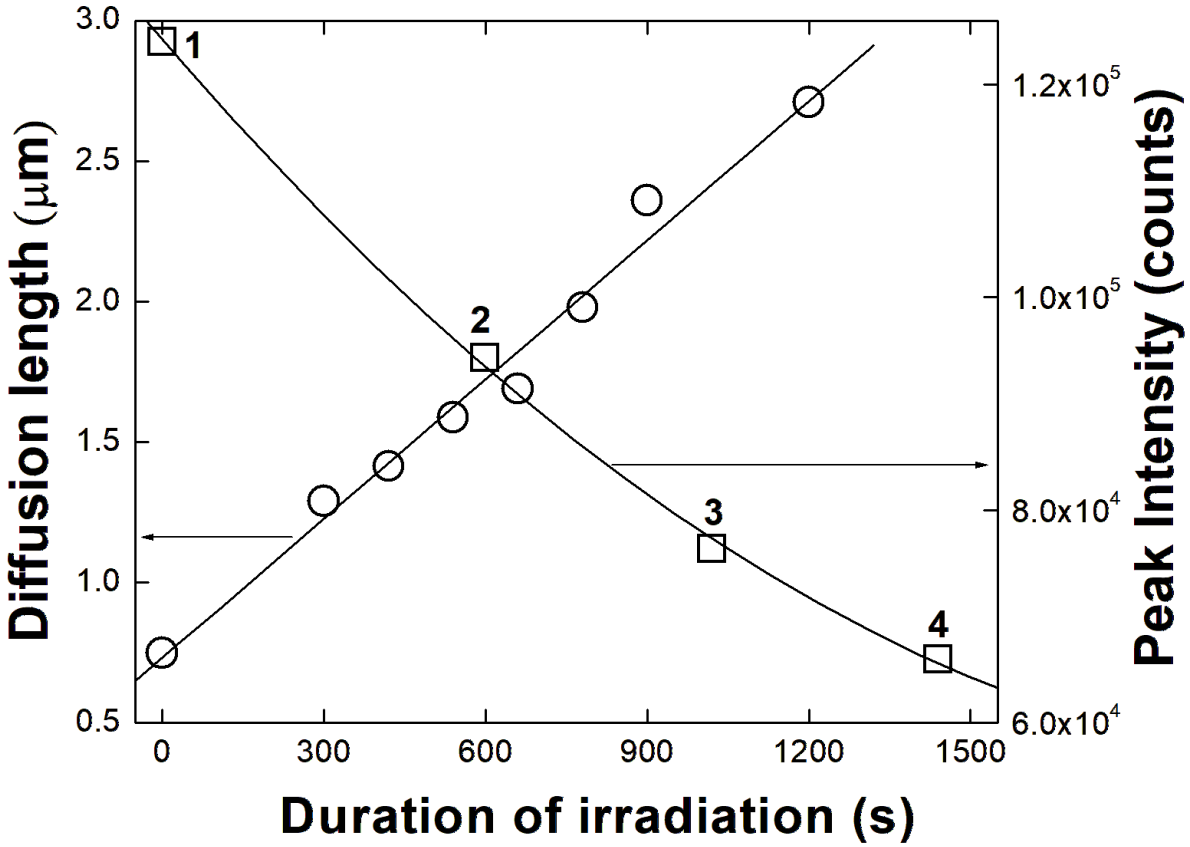
Diffusion length (μm)
Peak Intensity (counts)
Duration of irradiation (s)
3.0
2.5
2.0
1.5
1.0
0.5
0
300
600
900
1200
1500
1.2x10^5
1.0x10^5
8.0x10^4
6.0x10^4
1
2
3
4

Fig. 2

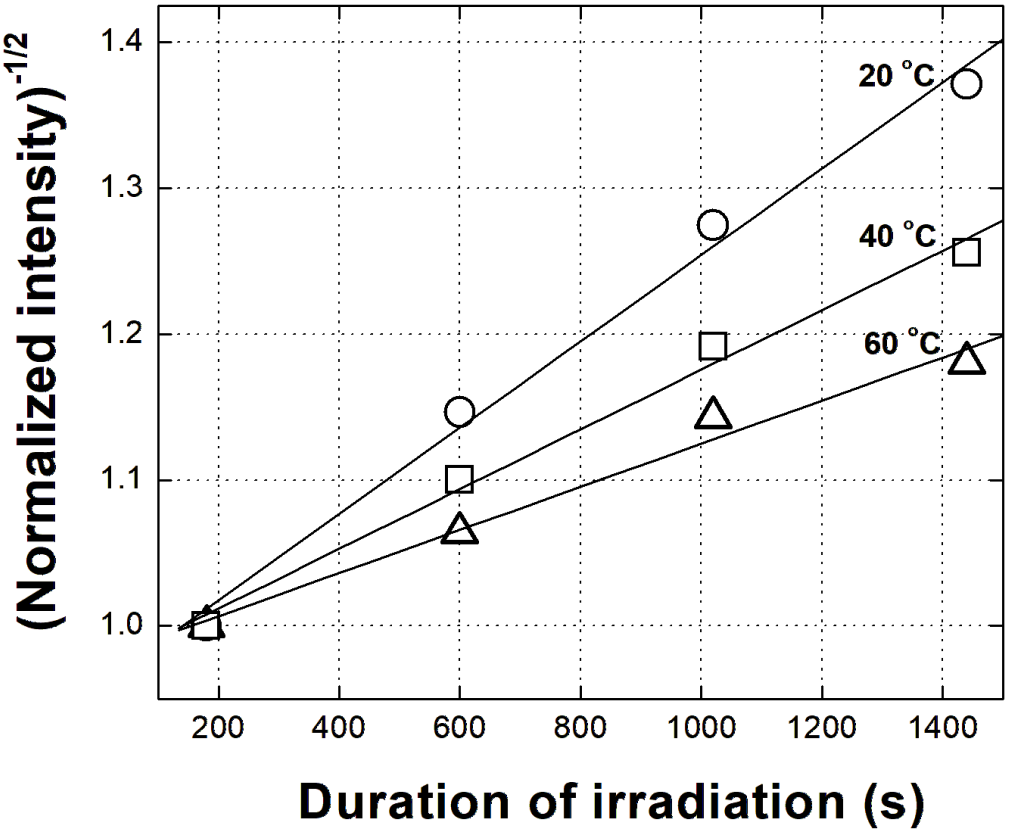
(Normalized intensity)$^{-1/2}$
1.4
1.3
1.2
1.1
1.0
200
400
600
800
1000
1200
1400
Duration of irradiation (s)
20 °C
40 °C
60 °C

Fig. 3

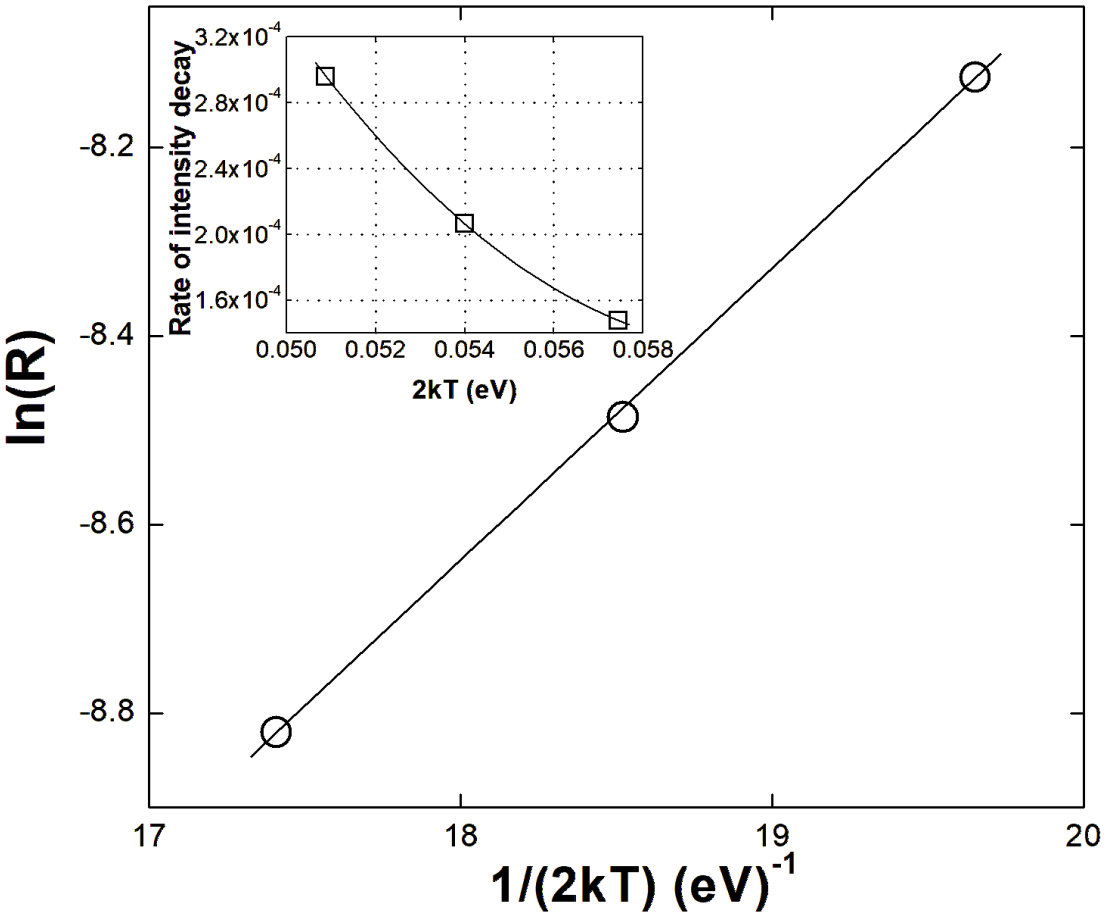
ln(R)
-8.2
-8.4
-8.6
-8.8
17
18
19
20
1/(2kT) (eV)-1
Rate of intensity decay
3.2x10-4
2.8x10-4
2.4x10-4
2.0x10-4
1.6x10-4
0.050
0.052
0.054
0.056
0.058
2kT (eV)

Fig. 4